Hybrid Density Functional Studies of Phenoxyl Free Radicals Modeling α-Tocopheroxyl

Patrick J. O'Malley

Department of Chemistry, UMIST, Manchester, M60 1QD U.K.

Received: March 12, 2002; In Final Form: August 2, 2002

Hybrid density functional calculations are used to study the geometry, spin density distribution and hyperfine coupling constants for a number of phenoxyl-type free radicals modeling the α-tocopheroxyl free radical. Stereoelectronic and inductive effects on the spin density distribution are investigated. Delocalization of the free radical spin density onto the para oxygen atom of the heterocyclic ring is allowed when the participating oxygen $2p_z$ orbital is held closely perpendicular to the main ring system as occurs for the α-tocopheroxyl radical. The resultant stabilization of the free radical enhances antioxidant (radical scavenging) activity. The effect of electron donating and electron withdrawing substituents on the heterocyclic ring is also studied with the carboxylate electron donating substituent, shown to increase delocalization of free radical unpaired spin. Calculated ^{1}H electron−nuclear hyperfine couplings are in good agreement with experimental determinations and calculated ^{13}C and ^{17}O anisotropic hyperfine coupling values are shown to provide an excellent direct guide to the spin density distribution of the phenoxyl free radicals studied.

Introduction

Deterioration in carbon-based materials is usually the result of a chemical reaction with oxygen of the environment. Oxidative degradation is now known to be due to free radical initiated autoxidation as originally proposed by Bäckström.[1] Following radical initiation, R•, autoxidation is propagated by rapid reaction with oxygen to generate the peroxyl radical (reaction 1)

$$R^{\bullet} + O_2 \rightarrow ROO^{\bullet} \quad (1)$$

This peroxyl radical can rapidly extract a hydrogen atom from another hydrocarbon molecule, RH, to generate a peroxide and another reactive free radical (reaction 2)

$$ROO^{\bullet} + RH \rightarrow ROOH + R^{\bullet} \quad (2)$$

This chain reaction can be broken by an appropriate antioxidant molecule which competes effectively with reaction 2 and generates a relatively unreactive free radical species. The widely used phenolic antioxidants (ArOH) function by competing with reaction 2 by donating a hydrogen atom to the reactive peroxyl free radical (reaction 3)

$$ROO^{\bullet} + ArOH \rightarrow ROOH + ArO^{\bullet} \quad (3)$$

The phenoxyl free radical generated is relatively stable, eventually decomposing into nonradical products and thereby breaks the chain of free radical generation which can lead to peroxidation and ultimately degrade polymers, lubricants, and food materials. The effectiveness of the phenol as an antioxidant will be directly related to the rate of reaction 3 above. Structure activity studies by Ingold et al.[2] have shown that the rate of this reaction is intimately linked to the nature of the substituents around the phenol; the rate being directly related to the to the ability of substituents to stabilize the developing spin density on the phenoxyl radical being formed.

Substituents which delocalize the developing electron spin will lower the barrier for reaction 3. The greater the delocalization in the transition state and the product phenoxyl, the greater the rate of reaction 3, and hence the greater the antioxidant activity. Nature has developed a highly efficient antioxidant system for biological systems. One of the most effective chain breaking lipid-soluble antioxidants is the phenolic compound α-tocopherol. QSAR studies[3] have shown that the

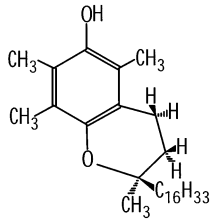

α-tocopherol

α-tocopherol structure and substituent pattern is well suited to perform as an effective chain-breaking antioxidant. More specifically, it has been proposed that the oxygen atom of the heterocyclic ring provides a very effective mechanism for delocalizing the phenoxyl spin density thereby stabilizing phenoxyl radical formation and increasing the rate of reaction 3. It has been proposed that the heterocyclic ring forces the 2p-type lone pair of electrons on the oxygen atom to remain closely perpendicular to the main phenol ring system thereby ensuring good overlap with the π-system electrons resulting in greater delocalization of the free radical spin density.

In addition, inductive effects of substituents situated next to the para oxygen have been postulated to influence the delocalization of the spin density. Electron withdrawing substituents neighboring the para oxygen are expected to decrease the ring-delocalization ability of the para oxygen in the free radical form thereby decreasing hydrogen atom transfer ability, whereas electron donating substituents are expected to enhance delocalization ability and hence increase hydrogen atom transfer ability.[4] Although the reactant phenols are amenable to a range of experimental studies, the free radical phenoxyl forms are not so amenable to experimental characterization. This is somewhat

10.1021/jp025754+ CCC: $22.00
Published on Web 11/02/2002

unfortunate as a thorough understanding of antioxidant function relies, as described above, on an understanding of the unpaired spin density distribution of the phenoxyl and its stabilization/destabilization on ring substitution. To probe this spin distribution electron paramagnetic resonance (EPR) has been used[4] to measure hyperfine couplings (hfcs) for phenoxyl radicals to help rationalize substituent effects. One is usually however limited to ^{1}H hyperfine couplings which are an indirect measure of the radicals π-electron spin density.[5] A more direct measure of the π-spin density could in principle be obtained by analysis of the ^{13}C and ^{17}O isotropic or anisotropic hyperfine couplings, but these have not been reported presumably because of difficulty of detection. Without such information, the complete spin density distribution for these phenoxyl-based free radicals cannot be attained experimentally.

Recent studies have shown the ability of hybrid density functional methods, in particular, B3LYP, to help characterize free radicals. In particular, excellent hyperfine coupling prediction for ^{1}H, ^{13}C, and ^{17}O nuclei have been demonstrated.[6] Only from such calculations can an accurate spin density distribution of free radicals be extracted.

Such calculations have also been used to study the OH bond dissociation energies of a variety of phenols and have developed a direct correlation between this parameter and antioxidant activity.[7]

Here, we use hybrid density functional calculations, unrestricted B3LYP, to predict the electronic structures and in particular the spin density distribution of phenoxyl free radicals relevant to the principal biological antioxidant α-tocopherol. In particular, we investigate the influence of streoelectronic and inductive effects on the phenoxyl spin density distribution.

Methods

The free radical forms of the phenol models used are shown in Figure 1. α-Tocopherol was modeled by 6-hydroxy-5,7,8-trimethylchroman (TOC). 2,3-Dihydro-5-hydroxy-2,4,6,7-tetramethylbenzofuran (STOC) was also investigated because of its observed high rate of free radical scavenging.[3] In addition, two phenols lacking the heterocyclic ring system but containing a methoxy substituent at the para position, 4-methoxy-2,3,5,6-tetramethylphenol (TEMP) and 4-methoxy-2,5,6-trimethylphenol (TRMP), were also studied. To examine the influence of inductive effects, the 6-hydroxy-2,5,7,8-tetramethylchroman-2-carboxylic acid (TOC-W) and the 6-hydroxy-2,5,7,8-tetramethylchroman-2-carboxylate anion radical (TOC-D) were also characterized. All calculations, including geometry optimization, were performed at the UB3LYP[8] level of theory using the Gaussian 98 program and the EPR-II basis set.[9]

Results and Discussion

Geometries. The principal optimized bond lengths for each radical studied are given in Figure 1. The geometries are typical of those predicted previously for simpler phenoxyl free radicals indicating "quinoid-like" structure with considerable double bond character for the C1−O bond.[10] As mentioned in the Introduction, the dihedral angle between the ring plane and the $2p_z$ orbital on the para oxygen has been proposed as a crucial factor in determining phenoxyl radical stability. The geometry optimized value of this angle is 0° for the TEMP radical, whereas it is 90° for the TRMP radical. The presence of methyl groups at both meta positions for TEMP pushes the methoxy group into an out of plane position. For the TOC and STOC

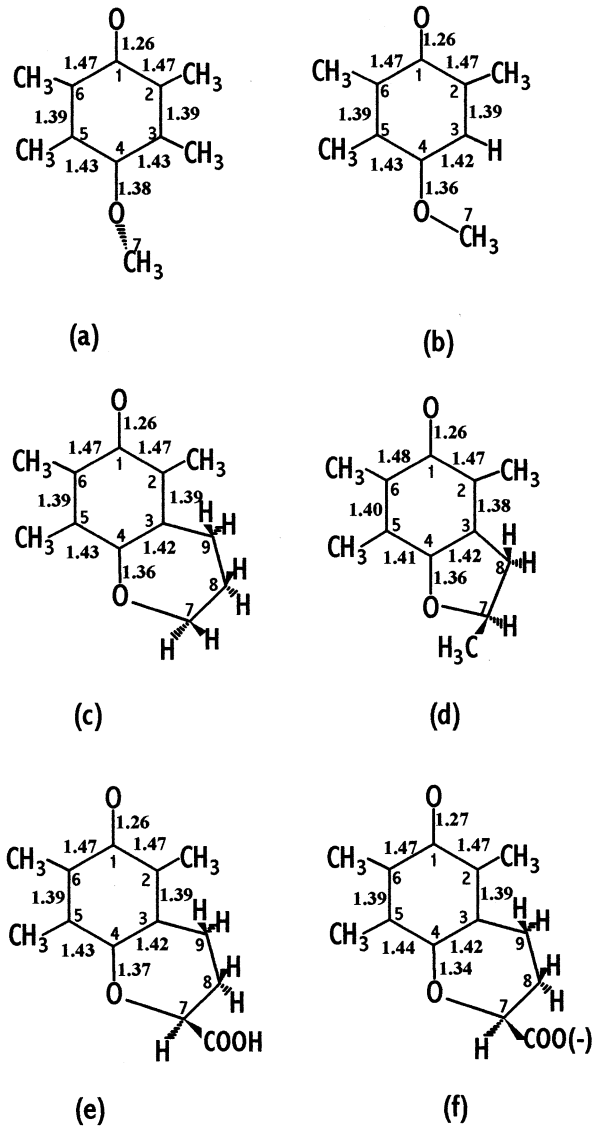

Figure 1. Structure and optimized bond lengths (Å) for the six free radicals studied. (a) TEMP, (b) TRMP, (c) TOC, (d) STOC, (e) TOC-W, and (f) TOC-D. The same, nonstandard numbering scheme is adopted throughout for ease of comparison.

radicals, the heterocyclic ring system forces this angle to remain close to perpendicular and the optimized values are 78° and 80° respectively. For TOC-W and TOC-D, these values are 78° and 82° respectively.

Spin Density Plots and Spin Populations. The unpaired spin density for the TEMP, TRMP, TOC, and STOC free radical contoured at 0.015 e/au is shown in Figure 2. Each radical displays an alternating pattern of spin density with high spin at the O1 and the C2 and C6 (ortho) and C4 (para) carbon positions. In general, for phenoxyl free radicals, substituents which can delocalize this spin density will stabilize the free radical. Such an effect is dominant for the para and ortho positions where the spin density is high. An oxygen substituent therefore at the para position can be expected to participate in the π-electron system and delocalize the spin density. This will depend however on the dihedral angle the oxygen p_z orbital makes with the π system. For the TRMP, TOC, and STOC radicals, the oxygen p_z orbital participates in the π-electron system, and hence, as the spin density plots of Figure 2 reveal, the spin density delocalizes onto this oxygen. For the TEMP radical, however, no significant delocalization is noted. This is

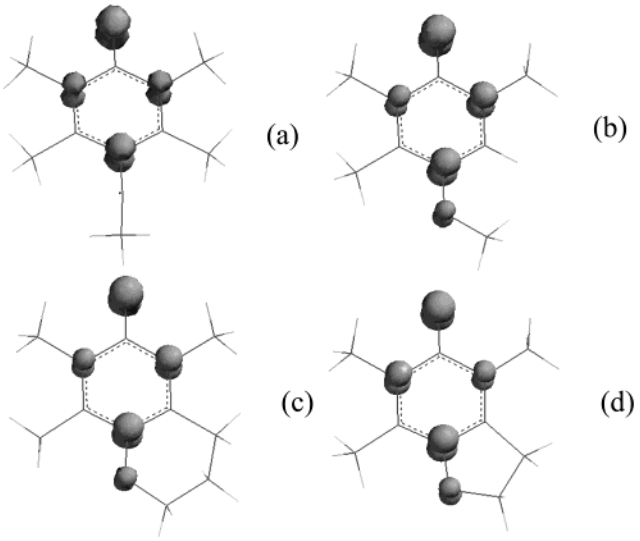

Figure 2. Unpaired spin density contours (0.015 e/au) for the first four free radicals of Figure 1. Orientation of radicals is as shown in Figure 1. (a) TEMP, (b) TRMP, (c) TOC, and (e) STOC.

due to the fact, as noted above, that the methoxy group is forced out of the ring plane by the two meta methyl groups thereby preventing conjugation of the oxygen 2p orbital with the π-electron system.

The calculated spin populations of Figure 3 give a more quantitative measure of such effects. Most notable is the spin population at the para oxygen for TEMP, which is 7−8 times smaller than for the other free radicals. TOC-W, with the electron withdrawing substituent, CO_2H, at position 7, shows a very similar spin population to TOC. The slightly increased ortho position values suggest a slightly more localized spin distribution compared with TOC that is in accord with its lower reaction rate with peroxyl free radicals.[4] Changing this heterocyclic ring substituent from CO_2H to CO_2^- has a much more dramatic effect on the spin populations. The CO_2^- group is by contrast strongly electron donating and as shown in Figure 3 leads to a more delocalized spin population on the phenoxyl ring. This would be expected to significantly enhance antioxidant activity. It is of interest to note that 6-hydroxy-2,5,7,8-tetramethylchroman-2-carboxylic acid is known[4b] to be a better food preservative than α-tocopherol. This cannot be explained on the basis of its unionized CO_2H form but at the pH of most food products the ionized CO_2^- is expected to exist and hence the superior antioxidant activity could be reasonably rationalized by the greater spin delocalization exhibited by the TOC-D free radical.

Hyperfine Couplings. As mentioned in the Introduction, hyperfine couplings measured using EPR spectroscopy can be used to get an experimental measurement of the spin density distribution of the radical. Studies of the ^{1}H nucleus have been reported in ref 4. Table 2 contains the calculated values for the six model radicals studied and compares them with those obtained experimentally for the same free radicals by Burton et al.[4b] Direct comparisons can be made for TOC, STOC, TEMP, and TRMP. Considering the isolated model nature, i.e., environmental effects are not accounted for, the agreement with experimentally reported couplings is good. The combined hyperfine couplings of the two ortho methyl groups is highest for the TEMP radical. This is in accord with the higher spin populations at these positions shown in Figure 3 pointing to a more localized spin density distribution for this radical form.

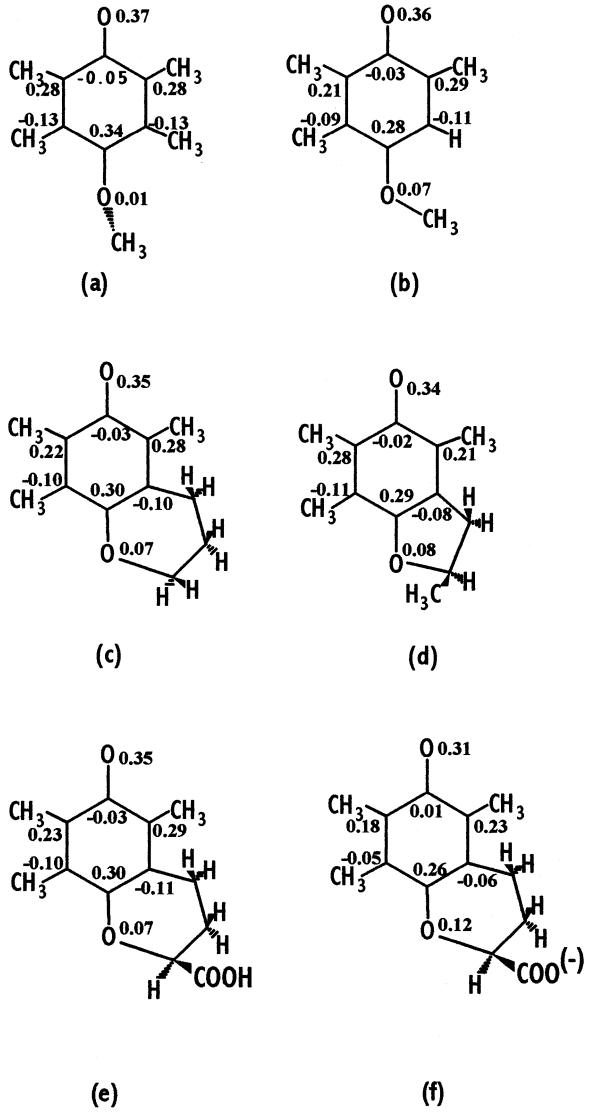

Figure 3. Mulliken unpaired spin populations for the free radicals of Figure 1.

TABLE 1: Calculated ^{1}H Isotropic Hyperfine Coupling Values (G) Compared with Experimental Determinations,[4b] in Brackets

radical	CH_3(6)	CH_3(2)	CH_3(7)	CH_2(7)
TOC	5.0 (4.6)	6.5 (6.0)		3.5 (3.3)
				−0.2 (<0.3)
STOC	6.6 (5.8)	5.1 (4.8)		2.9 (2.0)
TEMP	6.8 (6.2)	6.8 (6.2)	−0.4 (<0.1)	
TRMP	6.9 (5.5)	4.9 (4.5)	1.7 (2.0)	
TOC−W	5.1	6.7		3.1
TOC-D	3.5	5.0		5.0

For the other radicals, the spin density is extended on to the para oxygen atom, and hence, some spin density is removed from the ring system resulting in a reduction in spin density at the ortho carbon positions which leads to the reduced ^{1}H hyperfine couplings observed for the methyl groups attached to these positions. This effect is greatest for the TOC-D form. The ^{1}H hyperfine coupling values of the methyl group protons of TEMP and TRMP at position 7 have also been measured experimentally via EPR spectroscopy. For the TOC free radical, Burton et al.[4b] measured one relatively large proton coupling and deduced a much smaller proton coupling for the other. This is nicely born out by our calculations. Significant positive

TABLE 2: Calculated ^{13}C and ^{17}O Isotropic, A_{iso}, and Anisotropic, (T_{11}, T_{22}, and T_{33}) Hyperfine Coupling Values (MHz)

	A_{iso}					T_{11} T_{22} T_{33}				
rad.	$^{13}C(6)$	$^{13}C(2)$	$^{13}C(4)$	$^{17}O(1)$	$^{17}O(4)$	$^{13}C(6)$	$^{13}C(2)$	$^{13}C(4)$	$^{17}O(1)$	$^{17}O(4)$
TOC	16.4	21.3	29.3	−23.1	−11.6	31.8	40.6	51.8	−104.1	−32.5
						−16.4	−20.7	−26.4	51.9	15.7
						−15.4	−19.9	−25.4	52.1	16.8
STOC	21.3	15.5	27.2	−22.3	−12.6	40.2	31.2	50.8	−100.0	−36.1
						−19.7	−15.2	−26.0	49.9	17.5
						−20.5	−16.0	−24.9	50.1	18.6
TEMP	22.2	22.3	38.3	−23.9	−19.5	40.7	40.7	58.7	−109.5	−8.9
						−20.9	−19.8	−29.7	54.7	3.8
						−19.8	−20.9	−29.0	54.8	5.1
TRMP	16.2	21.9	28.4	−23.7	−10.7	31.7	41.8	50.1	−104.2	−31.4
						−16.4	−20.4	−24.6	54.7	16.3
						−15.4	−20.5	−25.5	54.8	15.1
TOC−W	16.9	22.2	30.5	−22.2	−10.8	32.3	41.9	52.7	−105.2	−30.5
						−16.7	−21.4	−26.9	52.7	15.8
						−15.6	−20.5	−26.8	52.5	14.7
TOC-D	11.0	14.9	20.4	−22.2	−16.6	25.2	32.2	44.9	−93.3	−47.4
						−13.0	−16.5	−23.1	46.8	24.3
						−12.3	−15.8	−21.8	46.5	23.1

hyperfine couplings are therefore calculated for the TRMP, STOC, and TOC free radicals at this position, Table 1. Excellent agreement with the experimental value recorded for TRMP is observed. For TEMP, only a small negative coupling is calculated in agreement with a small magnitude coupling measured experimentally. Unpaired spin density, giving rise to these couplings, arises at these protons via hyperconjugation with the O4 π-spin density. The absence of significant spin density at this position for TEMP precludes any hyperfine interaction for this free radical, whereas the presence of spin density at this position for the other systems, Figures 2 and 3, results in a sizable positive hyperfine coupling value for the protons involved.

Although the EPR experimental measurements have been limited for experimental reasons to the ^{1}H nucleus, as described above, Table 2 reveals that an excellent marker of the unpaired spin density distribution can be obtained from the magnitudes of the ^{17}O and ^{13}C nuclear hyperfine couplings. These hyperfine couplings require isotopic enrichment for their detection via EPR and provide a much more direct indicator of spin density distribution than the more easily measured ^{1}H couplings. The anisotropic principal hyperfine tensor values are directly proportional to the π-unpaired spin density surrounding the respective nuclei. The magnitude of the anisotropic values in Table 2 therefore reflect the spin population trend revealed in Figure 3. Of note is the smaller and larger magnitude values calculated at O4 for TEMP and TOC-D, respectively, when compared with the other free radicals. This reflects the absence of spin at this oxygen for TEMP and the presence of substantial spin for TOC-D, as revealed by Figures 2 and 3. It is also found that the anisotropic ^{13}C values for the TEMP radical at the ortho and para positions are larger than for the other free radical forms reflecting again the greater localization of spin density on the ring system for this radical. The isotropic ^{13}C and ^{17}O hyperfine couplings are indirectly related to the π-spin density. Isotropic hyperfine coupling arises from spin density directly at the nucleus in question and is due to spin polarization for a π-radical system as studied here. For the ^{13}C values, it can be seen that the isotropic hyperfine coupling is directly proportional to the π-spin density at the respective carbon. For ^{17}O, no such trend is found. For the O4 nucleus, the largest magnitude ^{17}O isotropic hyperfine coupling value is calculated for the TEMP free radical which has negligible π-spin density at the O4 position. The isotropic ^{17}O hyperfine coupling is known[5] to depend on the spin population of the neighboring atoms, C4 in this case. In essence, spin polarization of the CO sigma bond can be due to π-spin density at the carbon or oxygen atoms. For the TEMP free radical, a large π-spin population occurs at the C4 position. Hence, it would appear that the O4 ^{17}O isotropic hyperfine coupling is predominantly due to spin polarization by the C4 π-spin density thereby causing a sizable ^{17}O isotropic hyperfine coupling to arise for O4 even though the π-spin population on O4 is negligible. It may indicate that the nonplanar orientation of the methoxy group for TEMP enhances the spin polarization mechanism in the CO bond leading to the larger ^{17}O isotropic hyperfine coupling observed. Experimental determination of the ^{17}O isotropic hyperfine coupling for this nucleus would be of interest to confirm this proposal.

Conclusions

Hybrid density functional calculations on models of phenol-based antioxidants have shown that delocalization of the unpaired spin density distribution of the phenoxyl radical can be enhanced by a properly oriented oxygen substituent at the para position. If the oxygen susbstituent at this position is held such that the $2p_z$ orbital is perpendicular to the phenol ring plane, delocalization of spin density can occur in the free radical species. If however the 2p orbital on the oxygen is forced out of this perpendicular orientation, delocalization will gradually decrease until eventually becoming zero at 0°. This is the situation for 4-methoxy-2,3,5,6-tetramethylphenol, where no delocalization of spin density can occur and no enhanced stabilization of the phenoxyl free radical is expected. Substituents neighboring the para oxygen atom of the heterocyclic ring can also influence the spin density delocalization in the free radical form and hence influence hydrogen transfer ability. The presence of an electron donating carboxylate group at this position is predicted to significantly increase spin delocalization in the free radical form and hence increase hydrogen transfer ability. Hybrid density functional calculations of phenoxyl free radical properties provide a powerful new method of exploring the electronic configuration of such radicals, which are often difficult to investigate experimentally. The ability of hybrid density functional calculations to accurately model phenoxyl

free radical properties opens up a new avenue for understanding and predicting the antioxidant activities of novel antioxidant species.

References and Notes

(1) Bäckström, H. L. J. *J. Am. Chem. Soc*. **1927**, *49*, 1460.

(2) (a) Howard, J. A.; Ingold, K. U. *Can. J. Chem*. **1962**, *40*, 1851. (b) Howard, A. J.; Ingold, K. U. *Can. J. Chem*. **1964**, *42*, 1044. (c) Brownlie, I. T.; Ingold, K. U. *Can. J. Chem*. **1967**, *45*, 2419.

(3) (a) Bowry, V. W.; Ingold, K. U. *Acc. Chem. Res*. **1999**, *32*, 27. (b) van Acker, S. A. B. E.; Koymans, L. M. H.; Bast, A. *Free Radical Biol. Med*. **1993**, *15*, 311.

(4) (a) Burton, G.; Ingold, K. U. *Acc. Chem. Res.* **1986**, *19*, 194. (b) Burton, G. W.; Doba, T.; Gabe, E. J.; Hughes, F. L.; Prasad, L.; Ingold, K. U. *J. Am. Chem. Soc.* **1985**, *107*, 7053. (c) Mukai, K.; Tsuzuki, N.; Ouchi, S.; Fukuzawa, K. *Chem. Phys. Lipids* **1982**, *30*, 337. (d) Mukai, K.; Tsuzuki, N.; Ishizu, K.; Ouchi, S.; Fukuzawa, K. *Chem. Phys. Lipids* **1981**, *29*, 129.

(5) Gordy, W. *Theory and Applications of Electron Spin Resonance*; Wiley: New York, 1980.

(6) (a) Barone, V. In *Recent Advances in Density Functional Methods*; Chong, D. P., Ed.; World Scientific Publishing: Singapore, 1995. (b) Rega, N.; Cossi, M.; Barone, V. *J. Am. Chem. Soc.* **1998**, *120*, 5723. (c) O'Malley, P. J.; Collins, S. J. *Chem. Phys. Lett.* **1996**, *259*, 296−300. (d) O'Malley, P. J. *Chem. Phys. Lett.* **1996**, *262*, 797−801.

(7) (a) Wright, J. S.; Carpenter, D. J.; McKay, D. J.; Ingold, K. U. *J. Am. Chem. Soc.* **1997**, *119*, 4245. (b) Wright, J. S.; Johnson, E. R.; DiLabio, G. A. *J. Am. Chem. Soc*. **2001**, *123*, 1173.

(8) Becke, A. D. *J. Chem. Phys.* **1993**, *98*, 5648.

(9) Frisch, M. J.; Trucks, G. W.; Schlegel, H. B.; Scuseria, G. E.; Robb, M. A.; Cheeseman, J. R.; Zakrzewski, V. G.; Montgomery, J. A., Jr.; Stratmann, R. E.; Burant, J. C.; Dapprich, S.; Millam, J. M.; Daniels, A. D.; Kudin, K. N.; Strain, M. C.; Farkas, O.; Tomasi, J.; Barone, V.; Cossi, M.; Cammi, R.; Mennucci, B.; Pomelli, C.; Adamo, C.; Clifford, S.; Ochterski, J.; Petersson, G. A.; Ayala, P. Y.; Cui, Q.; Morokuma, K.; Malick, D. K.; Rabuck, A. D.; Raghavachari, K.; Foresman, J. B.; Cioslowski, J.; Ortiz, J. V.; Stefanov, B. B.; Liu, G.; Liashenko, A.; Piskorz, P.; Komaromi, I.; Gomperts, R.; Martin, R. L.; Fox, D. J.; Keith, T.; Al-Laham, M. A.; Peng, C. Y.; Nanayakkara, A.; Gonzalez, C.; Challacombe, M.; Gill, P. M. W.; Johnson, B. G.; Chen, W.; Wong, M. W.; Andres, J. L.; Head-Gordon, M.; Replogle, E. S.; Pople, J. A. *Gaussian 98*; Gaussian, Inc.: Pittsburgh, PA, 1998.

(10) Chipman, D. M.; Liu, R.; Zhou, X.; Pulay, P. *J. Chem. Phys*. **1994**, *100*, 5023.